PHYSICAL REVIEW C **96**, 041601(R) (2017)

Enhanced nucleon transfer in tip collisions of ^{238}U+^{124}Sn

Kazuyuki Sekizawa*
Faculty of Physics, Warsaw University of Technology, Ulica Koszykowa 75, 00-662 Warsaw, Poland
(Received 9 August 2017; revised manuscript received 9 October 2017; published 30 October 2017)

Multinucleon transfer processes in low-energy heavy ion reactions have attracted increasing interest in recent years aiming at the production of new neutron-rich isotopes. Clearly, it is an imperative task to further develop understanding of underlying reaction mechanisms to lead experiments to success. In this paper, from systematic time-dependent Hartree-Fock calculations for the ^{238}U+^{124}Sn reaction, it is demonstrated that transfer dynamics depend strongly on the orientations of ^{238}U, quantum shells, and collision energies. Two important conclusions are obtained: (i) Experimentally observed many-proton transfer from ^{238}U to ^{124}Sn can be explained by a multinucleon transfer mechanism governed by enhanced neck evolution in tip collisions; (ii) novel reaction dynamics are observed in tip collisions at energies substantially above the Coulomb barrier, where a number of nucleons are transferred from ^{124}Sn to ^{238}U, producing transuranium nuclei as primary reaction products, which could be a means to synthesize superheavy nuclei. Both results indicate the importance of the neck (shape) evolution dynamics, which are sensitive to orientations, shell effects, and collision energies, for exploring possible pathways to produce new unstable nuclei.

DOI: 10.1103/PhysRevC.96.041601

Introduction. Neck development is one of the fundamental degrees of freedom in nuclear dynamics. When a nucleus splits into two— nuclear fission [1,2]—the ways of evolving a neck characterize the fission outcomes such as kinetic and excitation energies as well as mass and charge of the fission products [3]. Since neck formation lowers the Coulomb barrier height [4–6], it significantly affects the fusion cross section. Moreover, the neck plays an important role in, e.g., nucleon exchanges and energy dissipation [7–15]. This work strengthens the importance of neck evolution dynamics in multinucleon transfer processes that could be a key element toward the synthesis of yet-unknown superheavy nuclei.

Recently, the multinucleon transfer reaction is considered as a promising means to produce new neutron-rich heavy nuclei and has been extensively studied [16–59]. In this context, among the pioneering experiments [60–68], Mayer *et al.* at GSI reported [69] measurements of production cross sections for lighter (target-like) fragments in ^{238}U-induced dissipative collisions with ^{110}Pd and ^{124}Sn targets, employing the inverse kinematics. It was observed that for the ^{238}U+^{124}Sn reaction at $E_{\text{c.m.}} \simeq 465$ MeV, up to around 15 protons are transferred from ^{238}U to ^{124}Sn, whereas the neutron number of the lighter fragments tends to be close to the neutron magic number, $N = 82$ [see Fig. 1(g) for the experimental data]. Similar shell effects were observed also for the ^{238}U+^{110}Pd reaction. The authors of Ref. [69] thus concluded that strong structural effects may be present in the ^{238}U-induced dissipative collisions, where the shell effects of $N = 82$ play a crucial role during the multiproton transfer processes. Even though the finding is fascinating, a clear theoretical explanation for this particular observation has not yet been given.

In this Rapid Communication, it is demonstrated, based on microscopic time-dependent Hartree-Fock (TDHF) calculations, that the observed multiproton transfer processes can be explained by characteristic neck evolution dynamics in tip collisions. Only in such a nuclear orientation does a thick and long neck develop in the course of the collision, and its subsequent rupture gives rise to the transfer of both neutrons and protons from ^{238}U to ^{124}Sn. Because of the dissipative character of the reaction, the reaction products are highly excited and secondary deexcitation processes affect significantly the production cross sections. It is shown that after the secondary particle evaporation, the neutron number of the lighter fragments tends to be close to the magic number, $N = 82$, explaining the experimental observation. To gain deeper insight into the reaction mechanism, collision energy dependence is also investigated for tip and side collisions, revealing a qualitative difference. In this paper, the importance of neck evolution dynamics in low-energy heavy ion reactions is highlighted.

Method. In this work, the TDHF theory is employed to unveil the mechanism of multinucleon transfer processes in the ^{238}U+^{124}Sn reaction. The theory is able to describe important dynamics during the collision, such as shape deformation of the composite system, nucleon exchanges, energy dissipation, shell effects, and so forth, without adjustable parameters. With the aid of the particle-number projection method [70], one can compute production cross sections for *primary* (excited) reaction products from the TDHF wave functions after collision [71]. Very recently, a method called TDHF+GEMINI was proposed [72], which combines the TDHF theory with a statistical compound-nucleus deexcitation model, GEMINI++ [73], that allows the evaluation of production cross sections for *secondary* reaction products after possible particle evaporation and/or fission. Those methods are used to make a comparison with the experimental data. (See, e.g., Refs. [74–78], for reviews, and Refs. [4–6,9–15,55,70,79–130], for recent applications of the TDHF theory.)

The TDHF calculations were performed using a parallel computational code [131], which has been successfully applied for various systems [71,72,131–136]. For the energy density

*Present address: Department of Physics, University of Washington, Seattle, WA 98195-1560, USA; sekizawa@uw.edu

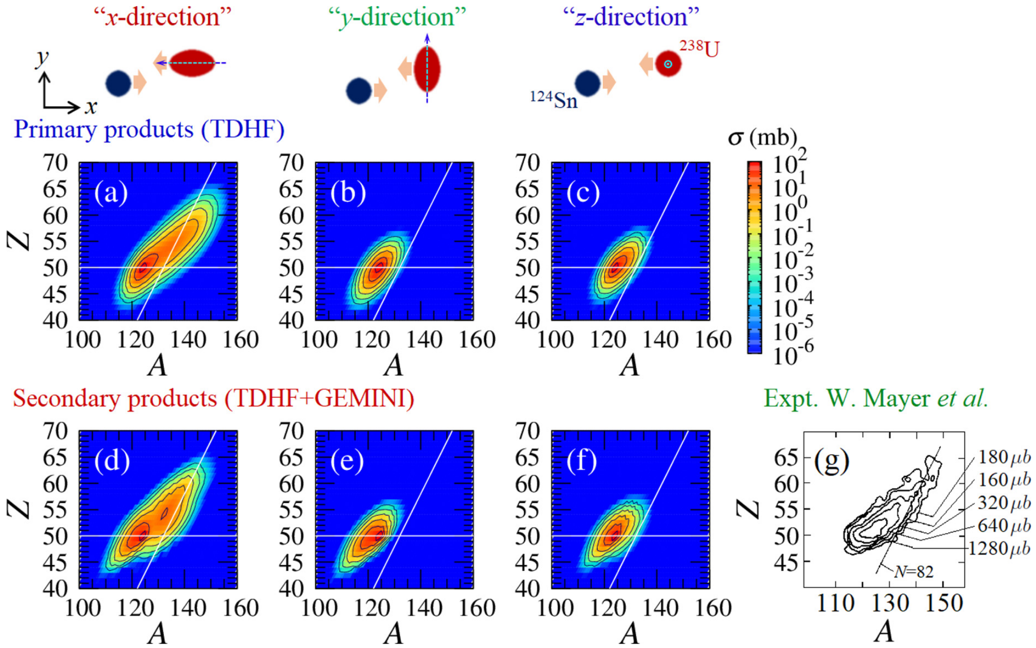

FIG. 1. Comparison of production cross sections for the lighter fragments in the ^{238}U+^{124}Sn reaction at $E_{\mathrm{c.m.}} \simeq 465$ MeV. (a)–(c): Cross sections for *primary* reaction products from TDHF. (d)–(f): Cross sections for *secondary* reaction products from TDHF+GEMINI. (g): Experimental data (for reaction products with energy losses $\geqslant 25$ MeV) reported in Ref. [69]. The magic numbers, $Z = 50$ and $N = 82$, are indicated by solid lines. The contour lines for the theoretical results in (a)–(f) correspond to 0.001, 0.01, 0.1, 1, 10, and 100 mb. At the top of the figure, the collision geometries examined are depicted, showing the x-direction case [for (a), (d)], the y-direction case [for (b), (e)], and the z-direction case [for (c), (f)]. The figure shown in (g) was taken from Ref. [69] with permission.

functional, the Skyrme SLy5 parameter set [137] was used. Static calculations were performed with a box of $(24\,\mathrm{fm})^3$ with an 0.8-fm mesh. The Hartree-Fock ground state of ^{124}Sn is of oblate shape with $\beta \simeq 0.11$ [71], while that of ^{238}U is of prolate shape with $\beta \simeq 0.27$ [134]. The TDHF calculations were performed with a three-dimensional box of $56\times56\times24$ fm^3 for noncentral collisions ($b \leqslant 10$ fm), while that was $72\times32\times24$ fm^3 for head-on collisions. Since ^{238}U exhibits a large prolate deformation, the calculations were performed taking three initial orientations of ^{238}U: the symmetry axis of ^{238}U is set parallel to the collision axis (x axis), parallel to the impact parameter vector (y axis), and perpendicular to the reaction plane (xy plane); while the symmetry axis of ^{124}Sn is always set perpendicular to the reaction plane. Those orientations will be called x-, y-, and z-direction cases, respectively, and are illustrated in the top part of Fig. 1. The same orientations were investigated for the ^{64}Ni+^{238}U reaction in Ref. [134]. The initial separation distance was set to 24 fm along the collision axis. Because of the excessively large total number of protons ($Z = 142$), fusion is no longer possible and binary reaction products were always observed. The time evolution was continued until the relative distance between the two fragments exceeded 28 fm.

The origin of many-proton transfer. Let us begin with clarifying the origin of the experimentally observed many-proton transfer in the ^{238}U+^{124}Sn reaction at $E_{\mathrm{c.m.}} \simeq 465$ MeV. Figure 1 exhibits the production cross sections for the lighter fragments in the A-Z plane. In the upper row, the cross sections for *primary* reaction products obtained from the TDHF calculations are shown; while, in the lower row, the cross sections for *secondary* reaction products from TDHF+GEMINI are shown. For TDHF+GEMINI, a simplified treatment that utilizes average excitation energy and angular momentum [72] was used, assuming that all the excitation energy evaluated from the TDHF wave function after collision gets thermalized forming a compound nucleus. Since a proper orientation average requires much computational effort, it has not been achieved and, instead, the contributions from the x-, y-, and z-direction cases are separately shown in Figs. 1(a) and 1(d), Figs. 1(b) and 1(e), and Figs. 1(c) and 1(f), respectively. The magic numbers, $Z = 50$ and $N = 82$, are indicated by solid lines. In Fig. 1(g), the measured cross sections reported in Ref. [69] are presented.

Let us first look at the experimental data shown in Fig. 1(g). The cross sections take the maximum value at around the initial mass and charge numbers of the target, $A = 124$ and $Z = 50$, as expected. As can be seen from the figure, the measured cross sections extend toward the right-top part in the A-Z plane, the direction increasing the mass and charge of the lighter fragments, meaning that many nucleons are transferred from ^{238}U to ^{124}Sn. One can also find that the neutron number of the lighter fragments tends to be around the magic number, $N = 82$. The authors of Ref. [69] therefore conjectured that this is a multiproton transfer process from ^{238}U to ^{124}Sn, under strong influence of the $N = 82$ shell closure.

Let us now turn to the theoretical results shown in Fig. 1 for primary and secondary products. From the figure, one can clearly see dramatic orientation dependence. Namely, when the symmetry axis of ^{238}U is set parallel to the collision axis [the x-direction case shown in Figs. 1(a) and 1(d)], the production cross sections extend widely in the A-Z plane. In contrast, when the symmetry axis of ^{238}U is set perpendicular to the collision axis [the y- and z-direction cases shown in Figs. 1(b) and 1(e) and Figs. 1(c) and 1(f), respectively], the cross sections distribute only narrowly around $A = 124$ and $Z = 50$. The important fact is that the cross sections for the many-nucleon transfer from ^{238}U to ^{124}Sn remain substantially large even after the secondary deexcitation processes, as shown in Fig. 1(d). Moreover, after the deexcitation processes, the cross sections look aligned along the neutron magic number, $N = 82$, consistent with the experimental observation.

Why does the amount of nucleon transfer depend so much on the orientation of ^{238}U? The answer lies in the remarkable difference of the neck evolution dynamics. In Fig. 2(a), snapshots of the density of the colliding nuclei at various times in head-on collisions of ^{238}U+^{124}Sn at $E_{\text{c.m.}} \simeq 465$ MeV are displayed, as an illustrative example. Time evolves from top to bottom rows, as indicated in each panel in zeptoseconds (1 zs = 10^{-21} s). In the left column, the result for the y-direction case (side collision) is shown; while the x-direction case (tip collision) is shown in the right column. From Fig. 2(a), one can clearly see that when ^{238}U collides from its tip on ^{124}Sn (right panels), two nuclei collide deeply ($t = 1.07$ zs) and then an elongated dinuclear system is formed, evolving a thick neck structure ($t = 1.6$–2.67 zs). Since the neck ruptures at a position closer to the heavier subsystem (incident ^{238}U in the right side), a number of nucleons inside the neck are subsequently absorbed by the smaller fragment ($t = 3.09$–3.26 zs). Similar dynamics have been observed also for noncentral collisions ($b \lesssim 3$ fm). On the other hand, when ^{238}U collides from its tip on ^{124}Sn (left panels), such a long neck is not developed ($t = 1.6$–2.29 zs) and only few nucleons are transferred on average. I must mention that the frozen Hartree-Fock treatment [138,139] offers an estimate of the Coulomb barrier height, which is $V_{\text{B}}^{\text{tip}} \simeq 410$ MeV (i.e., $E_{\text{c.m.}}/V_{\text{B}}^{\text{tip}} \simeq 1.13$) and $V_{\text{B}}^{\text{side}} \simeq 448$ MeV (i.e., $E_{\text{c.m.}}/V_{\text{B}}^{\text{side}} \simeq 1.04$) for the tip and side collisions, respectively, for the present system.

Summarizing, the present TDHF calculations and the analysis by TDHF+GEMINI indicate that what was observed experimentally is the tip-collision-induced many-nucleon transfer, which is induced by dynamics of a thick and long neck forming and breaking, followed by secondary evaporation processes.

Energy dependence of the reaction dynamics. One may ask about the energy dependence of the neck evolution dynamics. Namely, one may naively expect that, even in the side collision, similar multinucleon transfer processes via the elongated dinuclear system formation and its subsequent rupture may emerge at higher collision energies. In what follows, it is shown that it is not the case.

Figure 3 shows average numbers of nucleons of the heavier fragments [Figs. 3(a) and 3(b)] and the lighter fragments [Figs. 3(c) and 3(d)] as a function of the center-of-mass energy. Here only head-on collisions are investigated, taking two initial orientations of ^{238}U, the x- and y-direction cases, which, respectively, correspond to the tip and side collisions. From the figure, one can see that in the side collisions (blue crosses), the average number of nucleons of the fragments does not depend much on the collision energy. The only visible trend is a gradual decrease (increase) of the average number of nucleons in the heavier (lighter) fragment. The larger decrease seen in Fig. 3(a) as compared to the increase seen in Fig. 3(c) indicates that substantial prompt neutron emissions from ^{238}U took place during the collision at higher

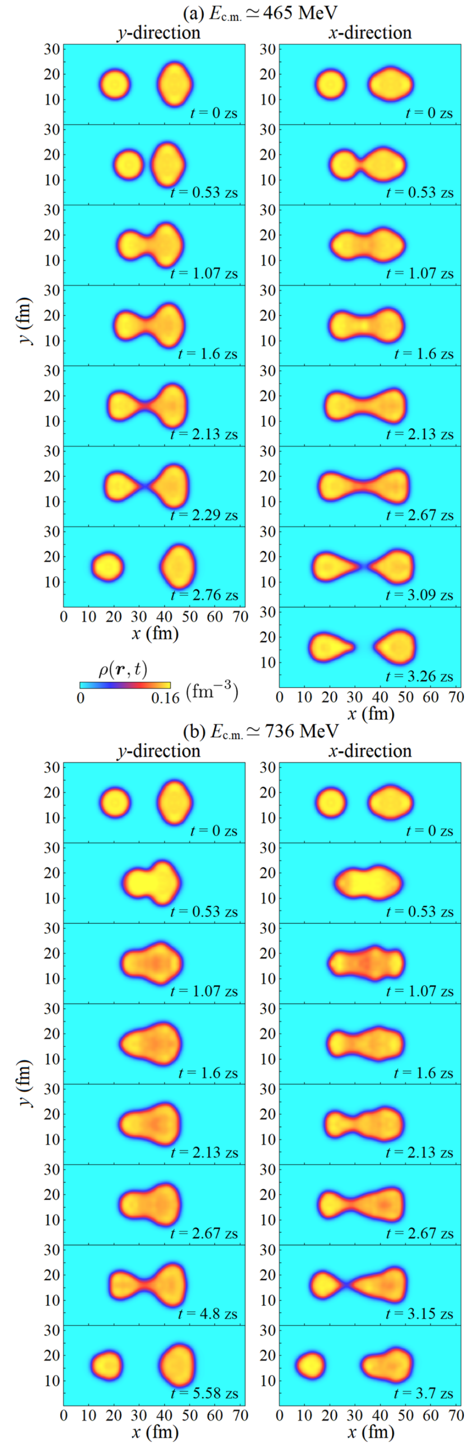

FIG. 2. Snapshots of the density in ^{238}U+^{124}Sn head-on collisions at $E_{\text{c.m.}} \simeq 465$ MeV (a) and 736 MeV (b).

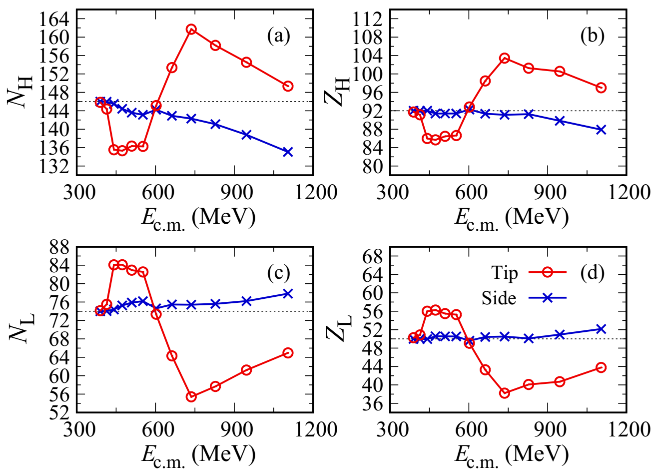

FIG. 3. TDHF results for head-on collisions of $^{238}U+^{124}Sn$ at various center-of-mass energies $E_{c.m.}$. Average numbers of neutrons and protons of the heavier fragments (N_H and Z_H) are shown in (a) and (b), respectively, while those of the lighter fragments (N_L and Z_L) are shown in (c) and (d), respectively. The results associated with tip (side) collisions are shown by read open circles (blue crosses). The neutron and proton numbers of the projectile and the target are indicated by horizontal dotted lines. The frozen Hartree-Fock treatment provides the Coulomb barrier height of $V_B^{tip} \simeq 410$ MeV and $V_B^{side} \simeq 448$ MeV for the tip and side collisions, respectively, for this system.

energies. In the left column of Fig. 2(b), an example of the reaction dynamics in the side collision at $E_{c.m.} \simeq 736$ MeV is shown. Nevertheless two nuclei collide so deeply and once form a compact shape without clear dinuclear structure ($t = 0.53$–2.13 zs), the system undergoes similar scission dynamics (2.67–5.58 zs), as was observed for lower energies [cf. the left column of Fig. 2(a)]. The results clearly indicate that the elongated neck structure is difficult to develop on the equatorial side of ^{238}U, even at higher energies substantially above the Coulomb barrier.

In stark contrast, in the tip collisions (red open circles), dramatic collision energy dependence is observed. Namely, at energy slightly above the Coulomb barrier ($E_{c.m.} \simeq 442$ MeV), the average number of nucleons shows a sudden jump, which corresponds to transfer of about 10 neutrons and 6 protons from ^{238}U to ^{124}Sn on average. Then it exhibits a prominent plateau pattern in the figure around ($N_H \simeq 136$, $Z_H \simeq 86$) and ($N_L \simeq 84$, $Z_L \simeq 56$) over a wide energy range of $442 \lesssim E_{c.m.} \lesssim 552$ MeV. The collision energy of $E_{c.m.} \simeq 465$ MeV that was investigated in the previous section actually belongs to this energy range. The latter process may be deemed as neck evolution dynamics under the influence of the quantum shells around $N = 82$ for the lighter fragment [cf. Fig. 3(c)] and $Z = 82$ for the heavier fragment [cf. Fig. 3(b)], although the values do not coincide exactly with those magic numbers. Note that in the plateau region the dynamics look similar to those shown in the right column of Fig. 2(a).

This is not the end of the story: i.e., as the collision energy increases further ($E_{c.m.} \gtrsim 552$ MeV), the plateau actually vanishes and even the direction of nucleon transfer reverses, resulting in many-nucleon transfer from light to heavy nuclei, which may be regarded as an *inverse* (antisymmetrizing) quasifission process [16,28–30,32–34,36,86]. At maximum, transfer of 16 neutrons and 11 protons from ^{124}Sn to ^{238}U is observed at around $E_{c.m.} \simeq 736$ MeV. The average primary reaction products correspond roughly to $^{93}_{38}Sr_{55}$ and $^{265}_{103}Lr_{162}$. The typical reaction dynamics of the latter process are displayed in the right column of Fig. 2(b). Since two nuclei collide so deeply, complex surface vibration modes are induced ($t = 1.07$ zs). As time evolves ($t = 1.6$–2.67 zs), a neck starts developing at a position closer to the smaller subsystem (incident ^{124}Sn in the left side), and eventually ruptures ($t = 3.15$ zs), producing a compact lighter fragment and a strongly deformed heaver fragment. It seems that there is complex interplay between density fluctuations, surface vibrations, and structural effects, e.g., probable shell effects around $Z = 40$, in the observed inverse quasifission process. It might also be related to dynamic clustering phenomena which were recently investigated in light systems within the TDHF approach [130]. To provide a conclusive explanation, however, further investigations are necessary, e.g., systematic calculations for other projectile-target combinations at a range of collision energies, along with investigations of structural properties of the composite system.

It should be noted that the observed inverse quasifission dynamics are different from those reported in, e.g., Ref. [34], where strong shell effects of ^{208}Pb induce nucleon transfer from ^{238}U to ^{248}Cm, and Ref. [86], where a "tip-on-side" configuration allows nucleon transfer from the tip of ^{232}Th to the side of ^{250}Cf. It would be interesting to explore similar inverse quasifission processes in, e.g., the $^{160}_{64}Gd_{96}+^{248}_{96}Cm_{152}$ reaction, where shell effects of $Z = 50$ (and possibly $N = 82$) or even $Z = 40$, as was observed in the present system, may induce production of superheavy nuclei; e.g., ${}_{64}Gd + {}_{96}Cm \rightarrow {}_{40}Zr + {}_{120}Ubn$. If one could take advantage of shell effects around ($Z = 114$ and $N = 184$) for heavier fragments and ($Z = 50$ and $N = 82$) for lighter fragments, the system may be able to access the island of stability: e.g., $^{186}_{74}W_{112}+^{248}_{96}Cm_{152} \rightarrow ^{136}_{56}Ba_{80}+^{298}_{114}Fl_{184}$. Of course, one has to carefully investigate the survival probability of the primary reaction products. One should also note that possible effects of two-body dissipations may be present in collisions well above the Coulomb barrier, which need to be addressed by, e.g., time-dependent density matrix (TDDM) [140] or molecular dynamics approaches (see, e.g., [54–56,58,59,141–145], and references therein). Nevertheless, the inverse quasifission process, assisted by the expected large (co)variances of fragment mass and charge distributions in such damped collisions [13,15,75], may be a possible way to produce yet-unknown superheavy nuclei.

Conclusions. Production of new neutron-rich heavy and superheavy isotopes is one of the hot topics in the nuclear physics community. In this paper, the reaction mechanism of the $^{238}U+^{124}Sn$ reaction has been investigated based on the microscopic framework of the time-dependent Hartree-Fock (TDHF) theory. From the systematic TDHF calculations for the reaction at various initial conditions, it has been demonstrated that the dynamics of neck formation and breaking, which in turn govern the amount and the direction of nucleon transfer, depend strongly on collision energy, quantum shells, and nuclear orientations. When ^{238}U collides from its tip on ^{124}Sn, a thick and long neck is developed and a number of nucleons inside the neck are transferred when it ruptures; whereas the neck formation is substantially hindered when ^{238}U collides from its side. The results have clearly shown that the experimentally observed many-proton transfer from ^{238}U to ^{124}Sn, whose mechanism was a mystery for over 30 years, may most likely be associated with the neck evolution dynamics in the tip collisions, followed by secondary evaporation processes. Moreover, at energies substantially above the Coulomb barrier, the emergence of novel reaction dynamics has been observed, where transuranium nuclei are produced as a result of many-nucleon transfer from ^{124}Sn to ^{238}U. The latter dynamics may be useful to create unknown superheavy nuclei. Both results strongly suggest that the neck evolution dynamics are vital degrees of freedom that should be appropriately taken into account in the reaction models for multinucleon transfer and quasifission processes at low energies around the Coulomb barrier. Furthermore, some symptom of proton-pair transfer in the ^{238}U+^{110}Pd and ^{238}U+^{124}Sn reactions was reported in Ref. [146], which can be addressed by extending the theoretical framework to include the pairing correlations [147–156]. Lastly, it should be emphasized that the TDHF approach can predict novel reaction dynamics in a nonempirical way, as demonstrated in this work. Therefore, further systematic TDHF calculations for various projectile-target combinations and collision energies have the potential to open new ways to reach neutron-rich heavy and superheavy nuclei that have never been produced to date.

Acknowledgments. The author wishes to thank P. Magierski (Warsaw University of Technology) for valuable comments on this article. The author acknowledges support of Polish National Science Centre (NCN) Grant, Decision No. DEC-2013/08/A/ST3/00708. This work used computational resources of the HPCI system (HITACHI SR16000/M1) provided by Information Initiative Center (IIC), Hokkaido University, through the HPCI System Research Projects (Project IDs: hp140010 hp150081, and hp170007). The author is grateful to Elsevier Ltd. for the permission to reuse the figure with modification.

[1] N. Bohr and J. A. Wheeler, The mechanism of nuclear fission, Phys. Rev. **56**, 426 (1939).
[2] D. L. Hill and J. A. Wheeler, Nuclear constitution and the interpretation of fission phenomena, Phys. Rev. **89**, 1102 (1953).
[3] N. Schunck and L. M. Robledo, Microscopic theory of nuclear fission: A review, Rep. Prog. Phys. **79**, 116301 (2016).
[4] A. S. Umar and V. E. Oberacker, Heavy-ion interaction potential deduced from density-constrained time-dependent Hartree-Fock calculation, Phys. Rev. C **74**, 021601(R) (2006).
[5] K. Washiyama and D. Lacroix, Energy dependence of the nucleus-nucleus potential close to the Coulomb barrier, Phys. Rev. C **78**, 024610 (2008).
[6] C. Simenel, M. Dasgupta, D. J. Hinde, and E. Williams, Microscopic approach to coupled-channels effects on fusion, Phys. Rev. C **88**, 064604 (2013).
[7] V. V. Volkov, Deep inelastic transfer reactions—The new type of reactions between complex nuclei, Phys. Rep. **44**, 93 (1978).
[8] H. Feldmeier, Transport phenomena in dissipative heavy-ion collisions: The one-body dissipation approach, Rep. Prog. Phys. **50**, 915 (1987).
[9] S. Ayik, K. Washiyama, and D. Lacroix, Fluctuation and dissipation dynamics in fusion reactions from a stochastic mean-field approach, Phys. Rev. C **79**, 054606 (2009).
[10] K. Washiyama, S. Ayik, and D. Lacroix, Mass dispersion in transfer reactions with a stochastic mean-field theory, Phys. Rev. C **80**, 031602(R) (2009).
[11] B. Yilmaz, S. Ayik, D. Lacroix, and K. Washiyama, Nucleon exchange mechanism in heavy-ion collisions at near-barrier energies, Phys. Rev. C **83**, 064615 (2011).
[12] B. Yilmaz, S. Ayik, D. Lacroix, and O. Yilmaz, Nucleon exchange in heavy-ion collisions within a stochastic mean-field approach, Phys. Rev. C **90**, 024613 (2014).
[13] S. Ayik, B. Yilmaz, and O. Yilmaz, Multinucleon exchange in quasifission reactions, Phys. Rev. C **92**, 064615 (2015).
[14] S. Ayik, O. Yilmaz, B. Yilmaz, and A. S. Umar, Quantal nucleon diffusion: Central collisions of symmetric nuclei, Phys. Rev. C **94**, 044624 (2016).
[15] S. Ayik, B. Yilmaz, O. Yilmaz, A. S. Umar, and G. Turan, Multi-nucleon transfer in central collisions of ^{238}U+^{238}U, Phys. Rev. C **96**, 024611 (2017).
[16] W. Loveland, A. M. Vinodkumar, D. Peterson, and J. P. Greene, Synthesis of heavy nuclei using damped collisions: A test, Phys. Rev. C **83**, 044610 (2011).
[17] E. M. Kozulin, E. Vardaci, G. N. Knyazheva, A. A. Bogachev, S. N. Dmitriev, I. M. Itkis, M. G. Itkis, A. G. Knyazev, T. A. Loktev, K. V. Novikov, E. A. Razinkov, O. V. Rudakov, S. V. Smirnov, W. Trzaska, and V. I. Zagrebaev, Mass distributions of the system ^{136}Xe+^{208}Pb at laboratory energies around the Coulomb barrier: A candidate reaction for the production of neutron-rich nuclei at $N = 126$, Phys. Rev. C **86**, 044611 (2012).
[18] J. V. Kratz, M. Schädel, and H. W. Gäggeler, Reexamining the heavy-ion reactions ^{238}U+^{238}U and ^{238}U+^{248}Cm and actinide production close to the barrier, Phys. Rev. C **88**, 054615 (2013).
[19] J. V. Kratz, W. Loveland, and K. J. Moody, Syntheses of transuranium isotopes with atomic numbers $\leqslant$103 in multi-nucleon transfer reactions, Nucl. Phys. A **944**, 117 (2015).
[20] J. S. Barrett, W. Loveland, R. Yanez, S. Zhu, A. D. Ayangeakaa, M. P. Carpenter, J. P. Greene, R. V. F. Janssens, T. Lauritsen, E. A. McCutchan, A. A. Sonzogni, C. J. Chiara, J. L. Harker, and W. B. Walters, ^{136}Xe+^{208}Pb reaction: A test of models of multinucleon transfer reactions, Phys. Rev. C **91**, 064615 (2015).
[21] A. Vogt, B. Birkenbach, P. Reiter, L. Corradi, T. Mijatović, D. Montanari, S. Szilner, D. Bazzacco, M. Bowry, A. Bracco, B. Bruyneel, F. C. L. Crespi, G. de Angelis, P. Désesquelles, J. Eberth, E. Farnea, E. Fioretto, A. Gadea, K. Geibel, A. Gengelbach, A. Giaz, A. Görgen, A. Gottardo, J. Grebosz, H. Hess, P. R. John, J. Jolie, D. S. Judson, A. Jungclaus,

W. Korten, S. Leoni, S. Lunardi, R. Menegazzo, D. Mengoni, C. Michelagnoli, G. Montagnoli, D. Napoli, L. Pellegri, G. Pollarolo, A. Pullia, B. Quintana, F. Radeck, F. Recchia, D. Rosso, E. Şahin, M. D. Salsac, F. Scarlassara, P.-A. Söderström, A. M. Stefanini, T. Steinbach, O. Stezowski, B. Szpak, Ch. Theisen, C. Ur, J. J. Valiente-Dobón, V. Vandone, and A. Wiens, Light and heavy transfer products in ^{136}Xe+^{238}U multinucleon transfer reactions, Phys. Rev. C **92**, 024619 (2015).

[22] Y. X. Watanabe, Y. H. Kim, S. C. Jeong, Y. Hirayama, N. Imai, H. Ishiyama, H. S. Jung, H. Miyatake, S. Choi, J. S. Song, E. Clement, G. de France, A. Navin, M. Rejmund, C. Schmitt, G. Pollarolo, L. Corradi, E. Fioretto, D. Montanari, M. Niikura, D. Suzuki, H. Nishibata, and J. Takatsu, Pathway for the Production of Neutron-Rich Isotopes around the $N = 126$ Shell Closure, Phys. Rev. Lett. **115**, 172503 (2015).

[23] T. Welsh, W. Loveland, R. Yanez, J. S. Barrett, E. A. McCutchan, A. A. Sonzogni, T. Johnson, S. Zhu, J. P. Greene, A. D. Ayangeakaa, M. P. Carpenter, T. Lauritsen, J. L. Harker, W. B. Walters, B. M. S. Amro, and P. Copp, Modeling multinucleon transfer in symmetric collisions of massive nuclei, Phys. Lett. B **771**, 119 (2017).

[24] C. H. Dasso, G. Pollarolo, and A. Winther, Systematics of Isotope Production with Radioactive Beams, Phys. Rev. Lett. **73**, 1907 (1994).

[25] C. H. Dasso, G. Pollarolo, and A. Winther, Particle evaporation following multinucleon transfer processes with radioactive beams, Phys. Rev. C **52**, 2264 (1995).

[26] R. Yanez and W. Loveland, Predicting the production of neutron-rich heavy nuclei in multinucleon transfer reactions using a semi-classical model including evaporation and fission competition, GRAZING-F, Phys. Rev. C **91**, 044608 (2015).

[27] V. Zagrebaev and W. Greiner, Unified consideration of deep inelastic, quasi-fission and fusion-fission phenomena, J. Phys. G: Nucl. Part. Phys. **31**, 825 (2005).

[28] V. I. Zagrebaev, Yu. Ts. Oganessian, M. G. Itkis, and W. Greiner, Superheavy nuclei and quasi-atoms produced in collisions of transuranium ions, Phys. Rev. C **73**, 031602(R) (2006).

[29] V. Zagrebaev and W. Greiner, Shell effects in damped collisions: A new way to superheavies, J. Phys. G: Nucl. Part. Phys. **34**, 2265 (2007).

[30] V. Zagrebaev and W. Greiner, Low-energy collisions of heavy nuclei: Dynamics of sticking, mass transfer and fusion, J. Phys. G: Nucl. Part. Phys. **34**, 1 (2007).

[31] V. Zagrebaev and W. Greiner, Production of New Heavy Isotopes in Low-Energy Multinucleon Transfer Reactions, Phys. Rev. Lett. **101**, 122701 (2008).

[32] V. Zagrebaev and W. Greiner, Synthesis of superheavy nuclei: A search for new production reactions, Phys. Rev. C **78**, 034610 (2008).

[33] V. I. Zagrebaev and W. Greiner, Production of heavy and superheavy neutron-rich nuclei in transfer reactions, Phys. Rev. C **83**, 044618 (2011).

[34] V. I. Zagrebaev and W. Greiner, Production of heavy trans-target nuclei in multinucleon transfer reactions, Phys. Rev. C **87**, 034608 (2013).

[35] V. I. Zagrebaev, B. Fornal, S. Leoni, and W. Greiner, Formation of light exotic nuclei in low-energy multinucleon transfer reactions, Phys. Rev. C **89**, 054608 (2014).

[36] V. I. Zagrebaev and W. Greiner, Cross sections for the production of superheavy nuclei, Nucl. Phys. A **944**, 257 (2015).

[37] A. V. Karpov and V. V. Saiko, Modeling near-barrier collisions of heavy ions based on a Langevin-type approach, Phys. Rev. C **96**, 024618 (2017).

[38] G. G. Adamian, N. V. Antonenko, and A. S. Zubov, Production of unknown transactinides in asymmetry-exit-channel quasifission reactions, Phys. Rev. C **71**, 034603 (2005).

[39] Yu. E. Penionzhkevich, G. G. Adamian, and N. V. Antonenko, Towards neutron drip line via transfer-type reactions, Phys. Lett. B **621**, 119 (2005).

[40] Yu. E. Penionzhkevich, G. G. Adamian, and N. V. Antonenko, Production of neutron-rich Ca isotopes in transfer-type reactions, Eur. Phys. J. A **27**, 187 (2006).

[41] Z.-Q. Feng, G.-M. Jin, and J.-Q. Li, Production of heavy isotopes in transfer reactions by collisions of ^{238}U+^{238}U, Phys. Rev. C **80**, 067601 (2009).

[42] G. G. Adamian, N. V. Antonenko, V. V. Sargsyan, and W. Scheid, Possibility of production of neutron-rich Zn and Ge isotopes in multinucleon transfer reactions at low energies, Phys. Rev. C **81**, 024604 (2010).

[43] G. G. Adamian, N. V. Antonenko, V. V. Sargsyan, and W. Scheid, Predicted yields of new neutron-rich isotopes of nuclei with $Z = 64$–80 in the multinucleon transfer reaction ^{48}Ca+^{238}U, Phys. Rev. C **81**, 057602 (2010).

[44] G. G. Adamian, N. V. Antonenko, and D. Lacroix, Production of neutron-rich Ca, Sn, and Xe isotopes in transfer-type reactions with radioactive beams, Phys. Rev. C **82**, 064611 (2010).

[45] M.-H. Mun, G. G. Adamian, N. V. Antonenko, Y. Oh, and Y. Kim, Production cross section of neutron-rich isotopes with radioactive and stable beams, Phys. Rev. C **89**, 034622 (2014).

[46] M.-H. Mun, G. G. Adamian, N. V. Antonenko, Y. Oh, and Y. Kim, Toward neutron-rich nuclei via transfer reactions with stable and radioactive beams, Phys. Rev. C **91**, 054610 (2015).

[47] L. Zhu, Z.-Q. Feng, and F.-S. Zhang, Production of heavy neutron-rich nuclei in transfer reactions within the dinuclear system model, J. Phys. G: Nucl. Part. Phys. **42**, 085102 (2015).

[48] L. Zhu, J. Su, W.-J. Xie, and F.-S. Zhang, Production of neutron-rich transcalifornium nuclei in ^{238}U-induced transfer reactions, Phys. Rev. C **94**, 054606 (2016).

[49] Z.-Q. Feng, Production of neutron-rich isotopes around $N = 126$ in multinucleon transfer reactions, Phys. Rev. C **95**, 024615 (2017).

[50] L. Zhu, J. Su, W.-J. Xie, and F.-S. Zhang, Theoretical study on production of heavy neutron-rich isotopes around the $N = 126$ shell closure in radioactive beam induced transfer reactions, Phys. Lett. B **767**, 437 (2017).

[51] C. Li, P. Wen, J. Li, G. Zhang, B. Li, and F.-S. Zhang, Production of heavy neutron-rich nuclei with radioactive beams in multinucleon transfer reactions, Nucl. Sci. Tech. **28**, 110 (2017).

[52] L. Zhu, F.-S. Zhang, P.-W. Wen, J. Su, and W.-J. Xie, Production of neutron-rich nuclei with $Z = 60$–73 in reactions induced by Xe isotopes, Phys. Rev. C **96**, 024606 (2017).

[53] K. Zhao, Z. Li, N. Wang, Y. Zhang, Q. Li, Y. Wang, and X. Wu, Production mechanism of neutron-rich transuranium nuclei in ^{238}U+^{238}U collisions at near-barrier energies, Phys. Rev. C **92**, 024613 (2015).

[54] C. Li, F. Zhang, J. Li, L. Zhu, J. Tian, N. Wang, and F.-S. Zhang, Multinucleon transfer in the ^{136}Xe+^{208}Pb reaction, Phys. Rev. C **93**, 014618 (2016).

[55] N. Wang and Lu Guo, New neutron-rich isotope production in ^{154}Sm+^{160}Gd, Phys. Lett. B **760**, 236 (2016).

[56] K. Zhao, Z. Li, Y. Zhang, N. Wang, Q. Li, C. Shen, Y. Wang, and X. Wu, Production of unknown neutron-rich isotopes in ^{238}U+^{238}U collisions at near-barrier energy, Phys. Rev. C **94**, 024601 (2016).

[57] G. A. Souliotis, M. Veselsky, G. Chubarian, L. Trache, A. Keksis, E. Martin, D. V. Shetty, and S. J. Yennello, Enhanced Production of Neutron-Rich Rare Isotopes in Peripheral Collisions at Fermi Energies, Phys. Rev. Lett. **91**, 022701 (2003).

[58] G. A. Souliotis, M. Veselsky, S. Galanopoulos, M. Jandel, Z. Kohley, L. W. May, D. V. Shetty, B. C. Stein, and S. J. Yennello, Approaching neutron-rich nuclei toward the r-process path in peripheral heavy-ion collisions at 15 MeV/nucleon, Phys. Rev. C **84**, 064607 (2011).

[59] P. N. Fountas, G. A. Souliotis, M. Veselsky, and A. Bonasera, Systematic study of neutron-rich rare isotope production in peripheral heavy-ion collisions below the Fermi energy, Phys. Rev. C **90**, 064613 (2014).

[60] E. K. Hulet, R. W. Lougheed, J. F. Wild, J. H. Landrum, P. C. Stevenson, A. Ghiorso, J. M. Nitschke, R. J. Otto, D. J. Morrissey, P. A. Baisden, B. F. Gavin, D. Lee, R. J. Silva, M. M. Fowler, and G. T. Seaborg, Search for Superheavy Elements in the Bombardment of ^{248}Cm with ^{48}Ca, Phys. Rev. Lett. **39**, 385 (1977).

[61] K. D. Hildenbrand, H. Freiesleben, F. Pühlhofer, W. F. W. Schneider, R. Bock, D. v. Harrach, and H. J. Specht, Reaction between ^{238}U and ^{238}U at 7.42 MeV/Nucleon, Phys. Rev. Lett. **39**, 1065 (1977).

[62] M. Schädel, J. V. Kratz, H. Ahrens, W. Brüchle, G. Franz, H. Gäggeler, I. Warnecke, G. Wirth, G. Herrmann, N. Trautmann, and M. Weis, Isotope Distributions in the Reaction of ^{238}U with ^{238}U, Phys. Rev. Lett. **41**, 469 (1978).

[63] P. Glässel, D. v. Harrach, Y. Civelekoglu, R. Männer, H. J. Specht, J. B. Wilhelmy, H. Freiesleben, and K. D. Hildenbrand, Three-Particle Exclusive Measurements of the Reactions ^{238}U+^{238}U and ^{238}U+^{248}Cm, Phys. Rev. Lett. **43**, 1483 (1979).

[64] H. Essel, K. Hartel, W. Henning, P. Kienle, H. J. Körner, K. E. Rehm, P. Sperr, W. Wagner, and H. Spieler, Charge and mass transfer in the reaction ^{136}Xe+^{208}Pb at energies close to the Coulomb barrier, Z. Phys. A **289**, 265 (1979).

[65] H. Freiesleben, K. D. Hildenbrand, F. Pühlhofer, W. F. W. Schneider, R. Bock, D. v. Harrach, and H. J. Specht, The reaction ^{238}U+^{238}U at 7.42 MeV/u, Z. Phys. A **292**, 171 (1979).

[66] M. Schädel, W. Brüchle, H. Gäggeler, J. V. Kratz, K. Sümmerer, G. Wirth, G. Herrmann, R. Stakemann, G. Tittel, N. Trautmann, J. M. Nitschke, E. K. Hulet, R. W. Lougheed, R. L. Hahn, and R. L. Ferguson, Actinide Production in Collisions of ^{238}U with ^{248}Cm, Phys. Rev. Lett. **48**, 852 (1982).

[67] K. J. Moody, D. Lee, R. B. Welch, K. E. Gregorich, G. T. Seaborg, R. W. Lougheed, and E. K. Hulet, Actinide production in reactions of heavy ions with ^{248}Cm, Phys. Rev. C **33**, 1315 (1986).

[68] R. B. Welch, K. J. Moody, K. E. Gregorich, D. Lee, and G. T. Seaborg, Dependence of actinide production on the mass number of the projectile: Xe+^{248}Cm, Phys. Rev. C **35**, 204 (1987).

[69] W. Mayer, G. Beier, J. Friese, W. Henning, P. Kienle, H. J. Körner, W. A. Mayer, L. Müller, G. Rosner, and W. Wagner, Structure effects in ^{238}U-induced dissipative collisions, Phys. Lett. B **152**, 162 (1985).

[70] C. Simenel, Particle Transfer Reactions with the Time-Dependent Hartree-Fock Theory Using a Particle Number Projection Technique, Phys. Rev. Lett. **105**, 192701 (2010).

[71] K. Sekizawa and K. Yabana, Time-dependent Hartree-Fock calculations for multinucleon transfer processes in ^{40,48}Ca+^{124}Sn, ^{40}Ca+^{208}Pb, and ^{58}Ni+^{208}Pb reactions, Phys. Rev. C **88**, 014614 (2013); **93**, 029902(E) (2016).

[72] K. Sekizawa, Microscopic description of production cross sections including deexcitation effects, Phys. Rev. C **96**, 014615 (2017).

[73] R. J. Charity, GEMINI: A Code to Simulate the Decay of a Compound Nucleus by a Series of Binary Decays, in *Joint ICTP-AIEA Advanced Workshop on Model Codes for Spallation Reactions*, Report INDC(NDC)-0530 (IAEA, Vienna, 2008), p. 139.

[74] J. W. Negele, The mean-field theory of nuclear structure and dynamics, Rev. Mod. Phys. **54**, 913 (1982).

[75] C. Simenel, Nuclear quantum many-body dynamics, Eur. Phys. J. A **48**, 152 (2012).

[76] T. Nakatsukasa, Density functional approaches to collective phenomena in nuclei: Time-dependent density functional theory for perturbative and non-perturbative nuclear dynamics, Prog. Theor. Exp. Phys. **2012**, 01A207 (2012).

[77] J. A. Maruhn, P.-G. Reinhard, P. D. Stevenson, and A. S. Umar, The TDHF code Sky3D, Comput. Phys. Commun. **185**, 2195 (2014).

[78] T. Nakatsukasa, K. Matsuyanagi, M. Matsuo, and K. Yabana, Time-dependent density-functional description of nuclear dynamics, Rev. Mod. Phys. **88**, 045004 (2016).

[79] L. Guo, J. A. Maruhn, and P.-G. Reinhard, Boost-invariant mean field approximation and the nuclear Landau-Zener effect, Phys. Rev. C **76**, 014601 (2007).

[80] C. Simenel, Ph. Chomaz, and G. de France, Fusion process studied with a preequilibrium giant dipole resonance in time-dependent Hartree-Fock theory, Phys. Rev. C **76**, 024609 (2007).

[81] L. Guo, J. A. Maruhn, P.-G. Reinhard, and Y. Hashimoto, Conservation properties in the time-dependent Hartree Fock theory, Phys. Rev. C **77**, 041301(R) (2008).

[82] A. S. Umar, V. E. Oberacker, and J. A. Maruhn, Neutron transfer dynamics and doorway to fusion in time-dependent Hartree-Fock theory, Eur. Phys. J. A **37**, 245 (2008).

[83] C. Golabek and C. Simenel, Collision Dynamics of Two ^{238}U Atomic Nuclei, Phys. Rev. Lett. **103**, 042701 (2009).

[84] K. Washiyama, D. Lacroix, and S. Ayik, One-body energy dissipation in fusion reactions from mean-field theory, Phys. Rev. C **79**, 024609 (2009).

[85] A. S. Umar, V. E. Oberacker, J. A. Maruhn, and P.-G. Reinhard, Microscopic calculation of precompound excitation energies for heavy-ion collisions, Phys. Rev. C **80**, 041601(R) (2009).

[86] D. J. Kedziora and C. Simenel, New inverse quasifission mechanism to produce neutron-rich transfermium nuclei, Phys. Rev. C **81**, 044613 (2010).

[87] A. S. Umar, V. E. Oberacker, J. A. Maruhn, and P.-G. Reinhard, Entrance channel dynamics of hot and cold fusion reactions leading to superheavy elements, Phys. Rev. C **81**, 064607 (2010).

[88] Y. Iwata, T. Otsuka, J. A. Maruhn, and N. Itagaki, Suppression of Charge Equilibration Leading to the Synthesis of Exotic Nuclei, Phys. Rev. Lett. **104**, 252501 (2010).

[89] V. E. Oberacker, A. S. Umar, J. A. Maruhn, and P.-G. Reinhard, Microscopic study of the ^{132,124}Sn+^{96}Zr reactions: Dynamic excitation energy, energy-dependent heavy-ion potential, and capture cross section, Phys. Rev. C **82**, 034603 (2010).
[90] Y. Iwata and J. A. Maruhn, Enhanced spin-current tensor contribution in collision dynamics, Phys. Rev. C **84**, 014616 (2011).
[91] M. Evers, M. Dasgupta, D. J. Hinde, D. H. Luong, R. Rafiei, R. du Rietz, and C. Simenel, Cluster transfer in the reaction ^{16}O+^{208}Pb at energies well below the fusion barrier: A possible doorway to energy dissipation, Phys. Rev. C **84**, 054614 (2011).
[92] A. S. Umar, V. E. Oberacker, J. A. Maruhn, and P.-G. Reinhard, Microscopic composition of ion-ion interaction potentials, Phys. Rev. C **85**, 017602 (2012).
[93] V. E. Oberacker, A. S. Umar, J. A. Maruhn, and P.-G. Reinhard, Dynamic microscopic study of pre-equilibrium giant resonance excitation and fusion in the reactions ^{132}Sn+^{48}Ca and ^{124}Sn+^{40}Ca, Phys. Rev. C **85**, 034609 (2012).
[94] C. Simenel, D. J. Hinde, R. du Rietz, M. Dasgupta, M. Evers, C. J. Lin, D. H. Luong, and A. Wakhle, Influence of entrance-channel magicity and isospin on quasi-fission, Phys. Lett. B **710**, 607 (2012).
[95] R. Keser, A. S. Umar, and V. E. Oberacker, Microscopic study of Ca + Ca fusion, Phys. Rev. C **85**, 044606 (2012).
[96] A. S. Umar, V. E. Oberacker, and C. J. Horowitz, Microscopic sub-barrier fusion calculations for the neutron star crust, Phys. Rev. C **85**, 055801 (2012).
[97] N. Loebl, A. S. Umar, J. A. Maruhn, P.-G. Reinhard, P. D. Stevenson, and V. E. Oberacker, Single-particle dissipation in a time-dependent Hartree-Fock approach studied from a phase-space perspective, Phys. Rev. C **86**, 024608 (2012).
[98] S. Fracasso, E. B. Suckling, and P. D. Stevenson, Unrestricted Skyrme-tensor time-dependent Hartree-Fock model and its application to the nuclear response from spherical to triaxial nuclei, Phys. Rev. C **86**, 044303 (2012).
[99] Y. Iwata, K. Iida, and N. Itagaki, Synthesis of thin, long heavy nuclei in ternary collisions, Phys. Rev. C **87**, 014609 (2013).
[100] C. I. Pardi and P. D. Stevenson, Continuum time-dependent Hartree-Fock method for giant resonances in spherical nuclei, Phys. Rev. C **87**, 014330 (2013).
[101] V. E. Oberacker and A. S. Umar, Microscopic analysis of sub-barrier fusion enhancement in ^{132}Sn+^{40}Ca versus ^{132}Sn+^{48}Ca, Phys. Rev. C **87**, 034611 (2013).
[102] C. Simenel, R. Keser, A. S. Umar, and V. E. Oberacker, Microscopic study of ^{16}O+^{16}O fusion, Phys. Rev. C **88**, 024617 (2013).
[103] A. S. Umar, C. Simenel, and V. E. Oberacker, Energy dependence of potential barriers and its effect on fusion cross sections, Phys. Rev. C **89**, 034611 (2014).
[104] C. Simenel and A. S. Umar, Formation and dynamics of fission fragments, Phys. Rev. C **89**, 031601(R) (2014).
[105] G. F. Dai, Lu Guo, E. G. Zhao, and S. G. Zhou, Effect of tensor force on dissipation dynamics in time-dependent Hartree-Fock theory, Sci. China Phys. Mech. Astron. **57**, 1618 (2014).
[106] T. K. Steinbach, J. Vadas, J. Schmidt, C. Haycraft, S. Hudan, R. T. deSouza, L. T. Baby, S. A. Kuvin, I. Wiedenhöver, A. S. Umar, and V. E. Oberacker, Sub-barrier enhancement of fusion as compared to a microscopic method in ^{18}O+^{12}C, Phys. Rev. C **90**, 041603(R) (2014).
[107] G.-F. Dai, Lu Guo, E.-G. Zhao, and S.-G. Zhou, Dissipation dynamics and spin-orbit force in time-dependent Hartree-Fock theory, Phys. Rev. C **90**, 044609 (2014).
[108] A. Wakhle, C. Simenel, D. J. Hinde, M. Dasgupta, M. Evers, D. H. Luong, R. du Rietz, and E. Williams, Interplay between Quantum Shells and Orientation in Quasifission, Phys. Rev. Lett. **113**, 182502 (2014).
[109] V. E. Oberacker, A. S. Umar, and C. Simenel, Dissipative dynamics in quasifission, Phys. Rev. C **90**, 054605 (2014).
[110] B. Schuetrumpf, K. Iida, J. A. Maruhn, and P.-G. Reinhard, Nuclear pasta matter for different proton fractions, Phys. Rev. C **90**, 055802 (2014).
[111] B. Schuetrumpf, M. A. Klatt, K. Iida, G. E. Schröder-Turk, J. A. Maruhn, K. Mecke, and P.-G. Reinhard, Appearance of the single gyroid network phase in “nuclear pasta” matter, Phys. Rev. C **91**, 025801 (2015).
[112] A. S. Umar and V. E. Oberacker, Time-dependent HF approach to SHE dynamics, Nucl. Phys. A **944**, 238 (2015).
[113] K. Hammerton, Z. Kohley, D. J. Hinde, M. Dasgupta, A. Wakhle, E. Williams, V. E. Oberacker, A. S. Umar, I. P. Carter, K. J. Cook, J. Greene, D. Y. Jeung, D. H. Luong, S. D. McNeil, C. S. Palshetkar, D. C. Rafferty, C. Simenel, and K. Stiefel, Reduced quasifission competition in fusion reactions forming neutron-rich heavy elements, Phys. Rev. C **91**, 041602(R) (2015).
[114] K. Washiyama, Microscopic analysis of fusion hindrance in heavy nuclear systems, Phys. Rev. C **91**, 064607 (2015).
[115] A. S. Umar, V. E. Oberacker, C. J. Horowitz, P.-G. Reinhard, and J. A. Maruhn, Swelling of nuclei embedded in neutron-gas and consequences for fusion, Phys. Rev. C **92**, 025808 (2015).
[116] A. S. Umar, V. E. Oberacker, and C. Simenel, Shape evolution and collective dynamics of quasifission in the time-dependent Hartree-Fock approach, Phys. Rev. C **92**, 024621 (2015).
[117] P. Goddard, P. Stevenson, and A. Rios, Fission dynamics within time-dependent Hartree-Fock: Deformation-induced fission, Phys. Rev. C **92**, 054610 (2015).
[118] P. Goddard, P. Stevenson, and A. Rios, Fission dynamics within time-dependent Hartree-Fock. II. Boost-induced fission, Phys. Rev. C **93**, 014620 (2016).
[119] D. Bourgin, C. Simenel, S. Courtin, and F. Haas, Microscopic study of ^{40}Ca+^{58,64}Ni fusion reactions, Phys. Rev. C **93**, 034604 (2016).
[120] P.-G. Reinhard, A. S. Umar, P. D. Stevenson, J. Piekarewicz, V. E. Oberacker, and J. A. Maruhn, Sensitivity of the fusion cross section to the density dependence of the symmetry energy, Phys. Rev. C **93**, 044618 (2016).
[121] B. Schuetrumpf, W. Nazarewicz, and P.-G. Reinhard, Time-dependent density functional theory with twist-averaged boundary conditions, Phys. Rev. C **93**, 054304 (2016).
[122] P. D. Stevenson, E. B. Suckling, S. Fracasso, M. C. Barton, and A. S. Umar, Skyrme tensor force in heavy ion collisions, Phys. Rev. C **93**, 054617 (2016).
[123] A. S. Umar, V. E. Oberacker, and C. Simenel, Fusion and quasifission dynamics in the reactions ^{48}Ca+^{249}Bk and ^{50}Ti+^{249}Bk using a time-dependent Hartree-Fock approach, Phys. Rev. C **94**, 024605 (2016).
[124] K. Vo-Phuoc, C. Simenel, and E. C. Simpson, Dynamical effects in fusion with exotic nuclei, Phys. Rev. C **94**, 024612 (2016).

[125] K. Godbey, A. S. Umar, and C. Simenel, Dependence of fusion on isospin dynamics, Phys. Rev. C **95**, 011601(R) (2017).
[126] V. Singh, J. Vadas, T. K. Steinbach, B. B. Wiggins, S. Hudan, R. T. deSouza, Z. Lin, C. J. Horowitz, L. T. Baby, S. A. Kuvin, V. Tripathi, I. Wiedenhöver, and A. S. Umar, Fusion enhancement at near and sub-barrier energies in ^{19}O+^{12}C, Phys. Lett. B **765**, 99 (2017).
[127] J. R. Stone, P. Danielewicz, and Y. Iwata, Proton and neutron density distributions at supranormal density in low- and medium-energy heavy-ion collisions, Phys. Rev. C **96**, 014612 (2017).
[128] C. Yu and Lu Guo, Angular momentum dependence of quasifission dynamics in the reaction ^{48}Ca+^{244}Pu, Sci. China Phys. Mech. Astron. **60**, 092011 (2017).
[129] A. S. Umar, C. Simenel, and W. Ye, Transport properties of isospin asymmetric nuclear matter using the time-dependent Hartree-Fock method, Phys. Rev. C **96**, 024625 (2017).
[130] B. Schuetrumpf and W. Nazarewicz, Cluster formation in pre-compound nuclei in the time-dependent framework, arXiv:1710.00579.
[131] K. Sekizawa, Multinucleon Transfer Reactions and Quasifission Processes in Time-Dependent Hartree-Fock Theory, Ph.D. thesis, University of Tsukuba, 2015.
[132] K. Sekizawa and K. Yabana, Particle-number projection method in time-dependent Hartree-Fock theory, Phys. Rev. C **90**, 064614 (2014).
[133] Sonika, B. J. Roy, A. Parmar, U. K. Pal, H. Kumawat, V. Jha, S. K. Pandit, V. V. Parkar, K. Ramachandran, K. Mahata, A. Pal, S. Santra, A. K. Mohanty, and K. Sekizawa, Multinucleon transfer study in ^{206}Pb(^{18}O, x) at energies above the Coulomb barrier, Phys. Rev. C **92**, 024603 (2015).
[134] K. Sekizawa and K. Yabana, Time-dependent Hartree-Fock calculations for multinucleon transfer and quasifission processes in the ^{64}Ni+^{238}U reaction, Phys. Rev. C **93**, 054616 (2016).
[135] K. Sekizawa and S. Heinz, Quasifission Dynamics and Stability of Superheavy Systems, Acta Phys. Pol. B Proc. Suppl. **10**, 225 (2017).
[136] B. J. Roy, Y. Sawant, P. Patwari, S. Santra, A. Pal, A. Kundu, D. Chattopadhyay, V. Jha, S. K. Pandit, V. V. Parkar, K. Ramachandran, K. Mahata, B. K. Nayak, A. Saxena, S. Kailas, T. N. Nag, R. N. Sahoo, P. P. Singh, and K. Sekizawa, Deep-inelastic multinucleon transfer processes in the ^{16}O+^{27}Al reaction, arXiv:1707.04164.
[137] E. Chabanat, P. Bonche, P. Haensel, J. Meyer, and R. Schaeffer, A Skyrme parametrization from subnuclear to neutron star densities Part II. Nuclei far from stabilities, Nucl. Phys. A **635**, 231 (1998); **643**, 441 (1998).
[138] V. Yu. Denisov and W. Nörenberg, Entrance channel potentials in the synthesis of the heaviest nuclei, Eur. Phys. J. A **15**, 375 (2002).
[139] C. Simenel, A. S. Umar, K. Godbey, M. Dasgupta, and D. J. Hinde, How the Pauli exclusion principle affects fusion of atomic nuclei, Phys. Rev. C **95**, 031601(R) (2017).
[140] M. Tohyama and A. S. Umar, Two-body dissipation effects on the synthesis of superheavy elements, Phys. Rev. C **93**, 034607 (2016).
[141] J. Aichelin, Quantum molecular dynamics—A dynamical microscopic n-body approach to investigate fragment formation and the nuclear equation of state in heavy ion collisions, Phys. Rep. **202**, 233 (1991).
[142] C. Hartnack, R. K. Puri, J. Aichelin, J. Konopka, S. A. Bass, H. Stöcker, and W. Greiner, Modelling the many-body dynamics of heavy ion collisions: Present status and future perspective, Eur. Phys. J. A **1**, 151 (1998).
[143] H. Feldmeier and J. Schnack, Molecular dynamics for fermions, Rev. Mod. Phys. **72**, 655 (2000).
[144] Y. Kanada-En'yo, M. Kimura, and A. Ono, Antisymmetrized molecular dynamics and its applications to cluster phenomena, Prog. Theor. Exp. Phys. **2012**, 01A202 (2012).
[145] G. Giuliani, H. Zheng, and A. Bonasera, The many faces of the (non-relativistic) Nuclear Equation of State, Prog. Part. Nucl. Phys. **76**, 116 (2014).
[146] W. Wagner, W. Mayer, G. Beier, J. Friese, W. Henning, P. Kienle, and H. J. Körner, Periodic multi-proton transfer strength in collisions between heavy nuclei, Phys. Lett. B **196**, 117 (1987).
[147] G. Scamps, D. Lacroix, G. F. Bertsch, and K. Washiyama, Pairing dynamics in particle transport, Phys. Rev. C **85**, 034328 (2012).
[148] G. Scamps and D. Lacroix, Effect of pairing on one- and two-nucleon transfer below the Coulomb barrier: A time-dependent microscopic description, Phys. Rev. C **87**, 014605 (2013).
[149] S. Ebata and T. Nakatsukasa, Pairing effects in nuclear fusion reaction, JPS Conf. Proc. **1**, 013038 (2014).
[150] S. Ebata and T. Nakatsukasa, Repulsive aspects of pairing correlation in nuclear fusion reaction, JPS Conf. Proc. **6**, 020056 (2015).
[151] Y. Hashimoto and G. Scamps, Gauge angle dependence in time-dependent Hartree-Fock-Bogoliubov calculations of ^{20}O+^{20}O head-on collisions with the Gogny interaction, Phys. Rev. C **94**, 014610 (2016).
[152] G. Scamps and Y. Hashimoto, Transfer probabilities for the reactions ^{14,20}O+^{20}O in terms of multiple time-dependent Hartree-Fock-Bogoliubov trajectories, Phys. Rev. C **96**, 031602(R) (2017).
[153] P. Magierski, K. Sekizawa, and G. Wlazłowski, Novel Role of Superfluidity in Low-Energy Nuclear Reactions, Phys. Rev. Lett. **119**, 042501 (2017).
[154] K. Sekizawa, P. Magierski, and G. Wlazłowski, Solitonic excitations in collisions of superfluid nuclei, PoS (INPC2016) 214.
[155] K. Sekizawa, G. Wlazłowski, and P. Magierski, Solitonic excitations in collisions of superfluid nuclei: A qualitatively new phenomenon distinct from the Josephson effect, arXiv:1705.04902.
[156] A. Bulgac and S. Jin, Dynamics of Fragmented Condensates and Macroscopic Entanglement, Phys. Rev. Lett. **119**, 052501 (2017).